Published in final edited form as:
J Biomech. 2012 August 9; 45(12): 2164–2170. doi:10.1016/j.jbiomech.2012.05.033.

Comparison of microCT and an inverse finite element approach for biomechanical analysis: Results in a MSC therapeutic system for fracture healing

Jared A. Weis[1], **Froilán Granero-Moltó**[2], **Timothy J. Myers**[2], **Lara Longobardi**[2], **Anna Spagnoli**[2,3], and **Michael I. Miga**[1,*]

[1]Department of Biomedical Engineering, Vanderbilt University, Nashville, TN 37232

[2]Department of Pediatrics, University of North Carolina at Chapel Hill, Chapel Hill, NC 27599

[3]Department of Biomedical Engineering, University of North Carolina at Chapel Hill, Chapel Hill, NC 27599

Abstract

An important concern in the study of fracture healing is the ability to assess mechanical integrity in response to candidate therapeutics in small-animal systems. In recent reports, it has been proposed that microCT image-derived densitometric parameters could be used as a surrogate for mechanical property assessment. Recently, we have proposed an inverse methodology that iteratively reconstructs the modulus of elasticity of the lumped soft callus/hard callus region by integrating both intrinsic mechanical property (from biomechanical testing) and geometrical information (from microCT) within an inverse finite element analysis (FEA) to define a callus quality measure. In this paper, data from a therapeutic system involving mesenchymal stem cells is analyzed within the context of comparing traditional microCT densitometric and mechanical property metrics. In addition, a novel multi-parameter regression microCT parameter is analyzed as well as our inverse FEA metric. The results demonstrate that the inverse FEA approach was the only metric to successfully detect both longitudinal and therapeutic responses. While the most promising microCT-based metrics were adequate at early healing states, they failed to track late-stage mechanical integrity. In addition, our analysis added insight to the role of MSCs by demonstrating accelerated healing and was the only metric to demonstrate therapeutic benefits at late-stage healing. In conclusion, the work presented here indicates that microCT densitometric parameters are an incomplete surrogate for mechanical integrity. Additionally, our inverse FEA approach is shown to be very sensitive and may provide a first-step towards normalizing the often challenging process of assessing mechanical integrity of healing fractures.

Keywords

Bone fracture healing; Mesenchymal stem cells; microCT; Material properties; Finite element analysis

[*]**Author for correspondence:** VU Station B, #351631, Nashville, TN 37235. Phone: 615-343-8336. Fax: 615-343-7919. michael.i.miga@vanderbilt.edu.

Conflict of Interest Statement None of the authors have any conflict of interest.

Introduction

Long bone fracture healing proceeds through the formation of a cartilaginous callus template that is progressively mineralized and replaced by bone which undergoes remodeling (Einhorn, 1998). There are approximately 7.9 million bone fractures that occur annually in the United States alone, with an approximate cost of $70 billion (Burge et al., 2007). However, 10-20 % of these fractures exhibit impaired healing, delayed union, or non-union (Marsh, 1998). Current methods of treatment include autograft, allograft, and pharmacological therapies. Recently, significant interest has been directed at mesenchymal stem cell (MSC) transplantation as a potential therapeutic treatment in bone fracture. Previous research has shown that MSC, infused systemically or implanted locally, migrate and home into damaged tissues including fractured bones to improve healing (Bruder et al., 1998a; Bruder et al., 1998b; Granero-Molto et al., 2008; Granero-Molto et al., 2009; Horwitz et al., 1999; Horwitz et al., 2001; Myers et al.; Oyama et al., 1999). In particular, MSC have been shown to migrate to and engraft at the fracture site and differentiate into mature mesenchymal cell types beneficially affecting fracture healing (Granero-Molto et al., 2009).

However, considerable uncertainty remains regarding true quantitative assessment of bone fracture healing. As the primary goal of fracture healing treatment is a return to load bearing function, mechanical integrity of the healing fracture callus is arguably the most important metric. Thus biomechanical testing (BMT) remains the gold standard for functional fracture healing assessment. However, biomechanical testing of fracture callus does not come without its own challenges. Classical mechanical analysis techniques use extrinsic force versus displacement data obtained from mechanical testing of homogeneous machined samples and analytic calculations based on specimen geometry to generate intrinsic material property information, such as elastic modulus. However, due to the atypical and inhomogeneous nature of the fracture callus, such machining and homogenization is not possible. Therefore, mechanical testing and theoretical calculations must be performed on the irregular and inhomogeneous specimen, for which a true closed-form solution does not exist, yielding whole-bone extrinsic material property metrics (such as apparent stiffness). Analytic calculations then rely on the assumption of a homogeneous and regular cross section. But because of the irregular geometry of the bone and callus, these calculations have been shown to be strongly biased by geometrical factors (van Lenthe et al., 2008) and are unable to generate accurate tissue-level intrinsic material properties. Thus, the current approach of determining extrinsic material properties as a biomechanical metric for fracture healing is lacking. Unfortunately, as a result, arguably one of the most important criteria, mechanical stability, is the least resolved with respect to fracture healing assessment.

Recent studies have suggested the use of microCT as not only a quantitative volumetric analysis method, but as a surrogate measure of mechanical function through correlation/multi-regression of microCT analysis parameters (Morgan et al., 2009; Nyman et al., 2009). A recent study utilizing these methods was able to explain 62% of the variability in maximum torque and 70% of the variability in torsional rigidity with microCT parameters used in multiple regression analyses (Morgan et al., 2009). However, this explanation is purely correlative in nature and does not directly address functionality of the healing callus tissue. These microCT metrics by design only provide quantification of volume and/or mineral density and therefore do not reflect the 3-dimensional mechanical connectivity of bone tissue within the callus. While the total volume and amount/density of mineral somewhat correlate with early stage healing progression, these are not the proper biomarkers to monitor as a determinant of fracture healing as they do not directly correspond to callus quality or mechanical function. While an imaging marker surrogate for mechanical function

is highly desirable, our hypothesis is that only through the direct analysis of force and displacement data can mechanical integrity be assessed.

Finite element analysis (FEA), a numerical simulation method in which an object is broken down into discreet sub-regions and mechanically simulated, has recently emerged as a method to analyze mechanical function and assess callus quality in fracture healing (Shefelbine et al., 2005; Weis et al., 2010). We have previously shown the capability of inverse finite element analysis as a method of jointly combining data from both microCT imaging and BMT, to detect changes in the elastic modulus of early stage normal bone fracture calluses in mice (Weis et al., 2010). Utilizing this inverse problem methodology, accurate predictions of intrinsic quality measures of the bone fracture callus tissue can be determined.

Within this study, we analyzed bone fracture callus tissue in mice either receiving or not receiving MSC transplantation through biomechanical analysis, microCT based analysis, and a novel inverse FEA modulus reconstruction procedure. The objectives of this study were to: 1) evaluate the discriminatory capability of analysis methods (biomechanical testing, microCT, and inverse FEA modulus reconstruction) in clearly highlighting differences between experimental and longitudinal groupings, 2) evaluate the sufficiency of microCT-derived measures as a surrogate for biomechanical analysis, and 3) monitor the longitudinal functional changes in callus tissue among experimental therapeutic groups.

Methods

Murine System

In previous work a murine tibia fracture healing system was developed to assess the behavior of bone fracture calluses with respect to mesenchymal stem cell (MSC) transplantation (Granero-Molto et al., 2009). In this follow-up study, 8-12 week old female FVB-NJ mice (Jackson Laboratories) were subjected to pin-stabilized tibial fracture utilizing a three-point bending impact device (total n = 17). At prescribed time points post-fracture (14 and 21 days), mice were euthanized and fractured tibias were prepared for analysis. Mice at each time point were divided into groups either receiving or not receiving therapeutic transplantation of 1×10^6 MSC via tail vein injection. Further details of the MSC transplantation system can be found in (Granero-Molto et al., 2009). MicroCT imaging data was collected and calibrated as previously described, using acquisition parameters of 55 kVP, 145 uA, 300 ms integration time, and 12 um voxel resolution (Scanco μCT 40) (Granero-Molto et al., 2009; Weis et al., 2010). Biomechanical testing and mechanical analysis were performed as previously described (Granero-Molto et al., 2009; Weis et al., 2010). Briefly, fracture calluses were loaded in tension while force and displacement were recorded until failure; biomechanical metrics of healing (peak force, stiffness, and toughness) were calculated as previously described (Weis et al., 2010).

Inverse Finite Element Analysis

Subject-specific FE models were generated by semi-automatic contour-based image segmentation and boundary surface extraction from microCT image data as previously described (Weis et al., 2010). The image segmentation and boundary surface extraction was performed for the callus tissue/air boundary as well as the cortical bone/callus tissue boundary, and the boundary description was used to create a tetrahedral FE mesh using custom-built mesh generation methods (Sullivan et al., 1997).

An inverse FEA procedure (as created in previous work (Weis et al., 2010)) was utilized to iteratively reconstruct the Young's modulus for callus material within the FE model. Briefly, the process begins with the creation of a subject specific Hookean linear elastic tissue

computer FE model of the bone/callus specimen generated from segmented microCT images. For each sample, an initial guess of the callus Young's modulus is assigned and displacement boundary conditions are applied that correspond to the experimental biomechanical testing protocol. From these simulations, the applied mechanical force can be estimated and compared to the empirical counterpart within a Levenberg-Marquardt non-linear optimization framework until a best fit is found (Weis et al., 2010). Details of the approach can be found in (Weis et al., 2010).

MicroCT Imaging Analysis Methods

A major goal of this study is to directly evaluate the sufficiency of microCT as a surrogate for mechanical integrity as compared to our novel inverse FEA approach within the context of a therapeutic MSC transplantation system. As a part of the study, the following standard microCT derived metrics were determined: total volume (TV) – defined as the volume of all voxels within the callus; bone volume (BV) – defined as the volume of voxels identified as bone by thresholding; callus mineralized volume fraction (BV/TV); tissue mineral density (TMD) – defined as the average voxel density (in g HA/m^3) of voxels within the BV component of the callus, standard deviation of mineral density (σ_{TMD}) – defined as the standard deviation of voxel density (in g HA/m^3) of voxels within the BV component of the callus; and bone mineral content (BMC) – defined as BV multiplied by TMD. A fixed global threshold of 25% of the maximum intensity value was selected to differentiate mineralized callus from non-mineralized callus, as suggested by the literature (Morgan et al., 2009).

A regression similar to that proposed by Morgan et al. (Morgan et al., 2009) was calculated retrospectively whereby a microCT-based multiple regression was used to predict mechanical properties from microCT measures. Briefly, the Statistics Toolbox in MATLAB was used to perform a multiple linear regression with TMD, BMC, BV/TV, and σTMD as predictors and stiffness as the response observation. Utilizing this methodology we obtain a metric representing mechanical stiffness that is derived purely from microCT data. This measure is equivalent in design to other microCT-to-BMT statistical models/correlations proposed in the literature (Morgan et al., 2009).

Comparisons Across and Among Analysis Metrics

Four unique data sets exist within the experimental mouse system data provided (two treatment cohorts - therapeutic and non-therapeutic, and at two different healing states - 14 days and 21 days) which leads to six unique comparisons among the groups. Comparisons by the proposed metrics should have some intuitive outcomes with respect to changes that are purely longitudinal in nature as well as supported outcomes from MSC transplantation based on the work in (Granero-Molto et al., 2009). With respect to longitudinal assessments, we should observe increased mechanical integrity within cohorts across time points. With respect to therapeutic assessments, based on (Granero-Molto et al., 2009) we would expect to observe increased mechanical integrity across treatment at similar time points. Comparing untreated early-stage to late-stage treated subjects should demonstrate combinatorial benefits. Lastly, comparing untreated late-stage to early-stage treated subjects should indicate equivalence based on (Granero-Molto et al., 2009) inferring that the early-stage treated subjects experienced improved healing due to the administration of MSC therapy.

One-way analysis of variance (ANOVA) was used to determine statistically significant metrics and unpaired Student's *t*-test was used pair-wise across and among longitudinal and therapeutic groups as a post test. Data are expressed as mean ± SD and statistical significance was set at $p<0.05$. Analysis metrics shown to be statistically significant by

ANOVA were subjected to pair-wise correlation analysis. Correlation coefficients were calculated by Pearson product-moment correlation coefficient analysis.

Results

MSC Effects on Callus microCT Metrics

Representative microCT image volumes from control non-recipient mice (NC) and MSC recipient mice (MSC) for both 14 and 21 days post-fracture are shown in Figure 1, and volumetric quantifications are reported in Figure 2. Statistical comparisons and associated p values are reported as compiled with all other metrics in Table 1. These data show that the degree of tissue mineralization is enhanced longitudinally in both NC and MSC groups and that MSC enhances this mineralization level at 14 days post-fracture but not at 21 days. Qualitatively demonstrated in the volumetric reconstructions in Figure 1, more mineralization as well as a greater degree of bridging bone is seen in the fracture callus both longitudinally and with MSC transplantation.

MSC Effects on Callus BMT Metrics

Biomechanical testing data from NC and MSC at 14 and 21 days post-fracture is shown in Figure 3. A wide variation in the curves is observed both among and across all testing groups representing a broad distribution of extrinsic biomechanical properties. Quantitative analysis of biomechanical testing metrics (ultimate load, toughness, and apparent stiffness) were generated and the results are shown in Figure 4. Statistical comparisons and associated p values are reported as compiled with all other metrics in Table 1. Reflecting the wide variation among biomechanical testing data, a statistically significant increase was observed for apparent stiffness only for NC mice from early to late-stage healing. These data show that extrinsic whole-bone BMT measures are enhanced longitudinally from 14 to 21 days post-fracture and that MSC transplantation enhances only some of these extrinsic properties at 14 days post-fracture but not at 21 days post-fracture. However, without accounting for the geometrical changes caused by time and MSC treatment on calluses, it is impossible to separate the enhancement in whole bone BMT behavior from either geometrical morphological changes or tissue-level mechanical improvement.

MSC Effects on Callus Inverse FEA Reconstructed Modulus

Finite element models were created as described and representative FE meshes are shown in Figure 1(E-H). Inverse FEA generated material property reconstructions were performed as described to generate estimations for the Young's modulus of the callus material. As shown in Figure 4, significant increases were observed for the inverse FEA modulus reconstructions for all important comparison groups longitudinally for both NC and MSC. Additionally, significant increases were observed for the inverse FEA modulus reconstructions in the case of MSC transplantation at both 14 days and 21 days post-fracture, representing an enhancement in the modulus of elasticity in calluses treated with MSC at both early and late-stage healing. Notably, a greater than 2 fold increase in inverse FEA reconstructed elastic modulus was observed at 21 days post-fracture for MSC transplantation as compared to control, which was the only metric analyzed that provided statistical significance at this time point. Statistical comparisons and associated p values are reported as compiled with all other metrics in Table 1.

Comparisons and Correlations among Analysis Metrics

Table 1 illustrates the compilation of the analysis metrics from this work. A legend of comparison metric names is displayed in the upper left hand corner of the matrix with quantitative p values associated with the pair-wise *t*-tests shown the matrix. The table is also

color-coded with green designating a statically significant difference and yellow designating no statistically significant difference. While the table yields considerable information, we draw attention to 3 interesting aspects. Outlined in magenta we see a clear comparison where a traditional biomechanical and microCT metric (stiffness and BV/TV) as well as the microCT-based stiffness regression fail to discriminate, whereas the inverse FEA reconstructed modulus and other traditional BMT and microCT metrics (peak force and TMD) show a statistically significant difference. Outlined in black, we see an interesting finding whereby the MSC treated 14 day post-fracture data is similar in tissue mineral density and mechanical properties to that of the untreated 21 day post-fracture. Lastly, circled in red, the comparison between 21 day post-fracture with and without MSC transplantation shows that our novel metric is the only one to identify a statistical difference.

Correlation analysis was performed pair-wise for each statistically significant metric and the correlation matrix is shown in Table 2. Moderate positive correlations between BMT and microCT were observed ranging from $r = 0.62$ to $r = 0.74$; however microCT metrics correlated weakest with the apparent stiffness parameter. Additionally, the inverse FEA estimated elastic modulus parameter was seen to correlate moderately with microCT derived measures and ultimate load.

Discussion

This study compared an inverse FEA elastic modulus reconstruction algorithm with both BMT and microCT derived metrics within the context of longitudinal changes in bone fracture healing and with therapeutic transplantation of MSC. Based on ANOVA, four of the six common microCT metrics demonstrated significance – bone volume-to-total volume ratio, tissue mineral density, standard deviation of tissue mineral density, and the microCT multi-parameter regression metric. With respect to mechanical property metrics, all showed some significance in monitoring changes within this experimental system – stiffness, toughness, peak force, and our novel inverse FEA modulus metric. One interesting finding is circled in black on Table 1 whereby early-stage treated mice demonstrated an equivalent mechanical property to their late-stage untreated counterparts. This suggests an accelerated rate of healing in response to MSC transplantation. It is also interesting to note in this comparison that the microCT regression metric assigned a statistically significant difference to this comparison, which in this case represents a failure as it is unsupported by the microCT, BMT, or inverse FEA modulus data. Another interesting finding is the red circled region of Table 1. This comparison at 21 days post-fracture with and without MSC transplantation indicates that our novel metric was the only one to register a statistical difference, whereas all microCT metrics failed this test. This result is troublesome with respect to considering microCT as a surrogate for mechanical function. Observing Figure 3b, a clear difference between these groups is supported. This indicates that while microCT measures could be a successful surrogate at early stage healing, its role throughout the continuum of healing is inadequate in these experiments. As we step back from this study, the inverse metric consistently passed all tests while the microCT metrics were of inconsistent veracity and at times failed. These data highlight the power of this analysis and the tenuous nature of microCT as a surrogate.

As reported, our results demonstrate that the inverse FEA reconstructed elastic modulus is a more sensitive measure of callus quality than BMT-only or microCT-only derived measures (including microCT-to-BMT regression based metrics). Throughout the range of comparisons, both traditional BMT and microCT derived measures were inconsistent across the comparisons conducted. As a result of this work, the suggestion that microCT measures be accepted as a surrogate for true mechanical functional analysis must be called into question. Furthermore, the mechanistic basis of the relationship between elastic modulus

derived via inverse FEA reconstructions and callus quality is quite clear from classical mechanics, whereas the relationship between microCT derived parameters is not. It is important to note that the combination of changes in intrinsic material properties as well as changes in callus geometry both strongly influence the overall quality of the fracture callus. However, the failure of densitometric parameters seen here is suggestive that improvements in callus quality are due to enhancement of the intrinsic material property of the callus (due to spatial arrangement/architecture rearrangement) instead of additive material geometrical benefits. Whereas the metric we have proposed is a measure that accounts for both the amount and arrangement of material and is directly relatable to classical mechanics. In addition, it is important to note that the microCT metrics analyzed reflect those of previous work (Morgan et al., 2009) and the murine system analyzed produced comparable correlations in both basic densitometric measures (Table 2, $r = 0.57$, stiffness vs. TMD) and multi-parameter regression measures (Table 2, $r = 0.75$, stiffness vs. μCT-reg). In similar approaches to ours, several authors have used bone geometry obtained from microCT to initialize FEM models with modulus values determined from the literature to run their models “forward” in order to predict mechanical behavior (Liu et al., 2006; Shefelbine et al., 2005). However, our approach represents a more “inverse” view of the problem that is capable of directly generating estimates of the intrinsic mechanical properties for the callus region through an inverse optimization model fitting procedure that combines microCT with biomechanical testing.

From our inverse FEA reconstruction data, we reach the supported conclusion that the elastic modulus of bone fracture callus tissue is gradually enhanced over time during early to late-stage fracture healing. Systemic transplantation of MSC accelerates the increase in callus elastic modulus. Over time, we expect this enhancement provided by MSC as compared to normal to gradually reduce as healing transitions into later stages, but further studies on late stage healing are needed to determine the exact timeline of MSC enhancement in callus tissue mechanical properties. Our results regarding the effects of MSC transplantation corroborate previous work (Granero-Molto et al., 2009), in that transplantation of MSC is seen to enhance fracture healing even in a normal fracture healing animal model, however it is important to note that this work advances the understanding of the biomechanical effects of MSC transplantation on healing callus tissue by demonstrating the increase in elastic modulus in response to therapy.

Lastly, it should be noted that there are several drawbacks to our current approach. Our methodology is currently unable to be directly translated to *in vivo* fracture healing assessment due to the direct biomechanical testing needed to provide mechanical information to the inverse FEA procedure. Also, our method is an intrinsic material property measurement and is intended to supplement but not replace whole callus mechanical measures (such as toughness) as geometry can play a significant role in clinical fracture stability. However, our procedure provides valuable and unique intrinsic callus mechanical property information necessary for assessment of experimental fracture healing due to therapeutic or genetic manipulations. Additionally, our method homogenizes the callus and considers the callus to be the combined soft and hard callus regions in order to report an intuitive measure of the overall mechanical integrity of the healing tissue. Also, the material simplification through the use of an assumed linear elastic constitutive law yields an inherently limited material model. But it should be noted that the goal of this study was to generate material property information based on an assumed material model that was capable of accurately discriminating longitudinal and therapeutic groupings, not to generate the most accurate multi-physics model of a bone fracture callus system.

Acknowledgments

This work was supported by a National Institutes of Health Grant 5R01DK070929-02 (to A.S.). We also acknowledge the technical support of the Vanderbilt Institute of Imaging Science at Vanderbilt University and the Biomedical Research Imaging Center at University of North Carolina at Chapel Hill.

References

Bruder SP, Jaiswal N, Ricalton NS, Mosca JD, Kraus KH, Kadiyala S. Mesenchymal stem cells in osteobiology and applied bone regeneration. Clin Orthop Relat Res. 1998a:S247–256. [PubMed: 9917644]

Bruder SP, Kraus KH, Goldberg VM, Kadiyala S. The effect of implants loaded with autologous mesenchymal stem cells on the healing of canine segmental bone defects. J Bone Joint Surg Am. 1998b; 80:985–996. [PubMed: 9698003]

Burge R, Dawson-Hughes B, Solomon DH, Wong JB, King A, Tosteson A. Incidence and economic burden of osteoporosis-related fractures in the United States, 2005-2025. J Bone Miner Res. 2007; 22:465–475. [PubMed: 17144789]

Einhorn TA. The cell and molecular biology of fracture healing. Clinical Orthopaedics and Related Research. 1998:S7–S21. [PubMed: 9917622]

Granero-Molto F, Weis JA, Longobardi L, Spagnoli A. Role of mesenchymal stem cells in regenerative medicine: application to bone and cartilage repair. Expert Opin Biol Ther. 2008; 8:255–268. [PubMed: 18294098]

Granero-Molto F, Weis JA, Miga MI, Landis B, Myers TJ, O'Rear L, Longobardi L, Jansen ED, Mortlock DP, Spagnoli A. Regenerative effects of transplanted mesenchymal stem cells in fracture healing. Stem Cells. 2009; 27:1887–1898. [PubMed: 19544445]

Horwitz EM, Prockop DJ, Fitzpatrick LA, Koo WW, Gordon PL, Neel M, Sussman M, Orchard P, Marx JC, Pyeritz RE, Brenner MK. Transplantability and therapeutic effects of bone marrow-derived mesenchymal cells in children with osteogenesis imperfecta. Nat Med. 1999; 5:309–313. [PubMed: 10086387]

Horwitz EM, Prockop DJ, Gordon PL, Koo WW, Fitzpatrick LA, Neel MD, McCarville ME, Orchard PJ, Pyeritz RE, Brenner MK. Clinical responses to bone marrow transplantation in children with severe osteogenesis imperfecta. Blood. 2001; 97:1227–1231. [PubMed: 11222364]

Liu XS, Sajda P, Saha PK, Wehrli FW, Guo XE. Quantification of the roles of trabecular microarchitecture and trabecular type in determining the elastic modulus of human trabecular bone. J Bone Miner Res. 2006; 21:1608–1617. [PubMed: 16995816]

Marsh D. Concepts of fracture union, delayed union, and nonunion. Clinical Orthopaedics and Related Research. 1998:S22–S30. [PubMed: 9917623]

Morgan EF, Mason ZD, Chien KB, Pfeiffer AJ, Barnes GL, Einhorn TA, Gerstenfeld LC. Micro-computed tomography assessment of fracture healing: relationships among callus structure, composition, and mechanical function. Bone. 2009; 44:335–344. [PubMed: 19013264]

Myers TJ, Granero-Molto F, Longobardi L, Li T, Yan Y, Spagnoli A. Mesenchymal stem cells at the intersection of cell and gene therapy. Expert Opin Biol Ther. 10:1663–1679. [PubMed: 21058931]

Nyman JS, Munoz S, Jadhav S, Mansour A, Yoshii T, Mundy GR, Gutierrez GE. Quantitative measures of femoral fracture repair in rats derived by micro-computed tomography. Journal of biomechanics. 2009; 42:891–897. [PubMed: 19281987]

Oyama M, Tatlock A, Fukuta S, Kavalkovich K, Nishimura K, Johnstone B, Robbins PD, Evans CH, Niyibizi C. Retrovirally transduced bone marrow stromal cells isolated from a mouse model of human osteogenesis imperfecta (oim) persist in bone and retain the ability to form cartilage and bone after extended passaging. Gene Ther. 1999; 6:321–329. [PubMed: 10435082]

Shefelbine SJ, Simon U, Claes L, Gold A, Gabet Y, Bab I, Muller R, Augat P. Prediction of fracture callus mechanical properties using micro-CT images and voxel-based finite element analysis. Bone. 2005; 36:480–488. [PubMed: 15777656]

Sullivan JM, Charron G, Paulsen KD. A three-dimensional mesh generator for arbitrary multiple material domains. Finite Elements in Analysis and Design. 1997; 25:219–241.

van Lenthe GH, Voide R, Boyd SK, Muller R. Tissue modulus calculated from beam theory is biased by bone size and geometry: implications for the use of three-point bending tests to determine bone tissue modulus. Bone. 2008; 43:717–723. [PubMed: 18639658]

Weis JA, Miga MI, Granero-Molto F, Spagnoli A. A finite element inverse analysis to assess functional improvement during the fracture healing process. Journal of biomechanics. 2010; 43:557–562. [PubMed: 19875119]

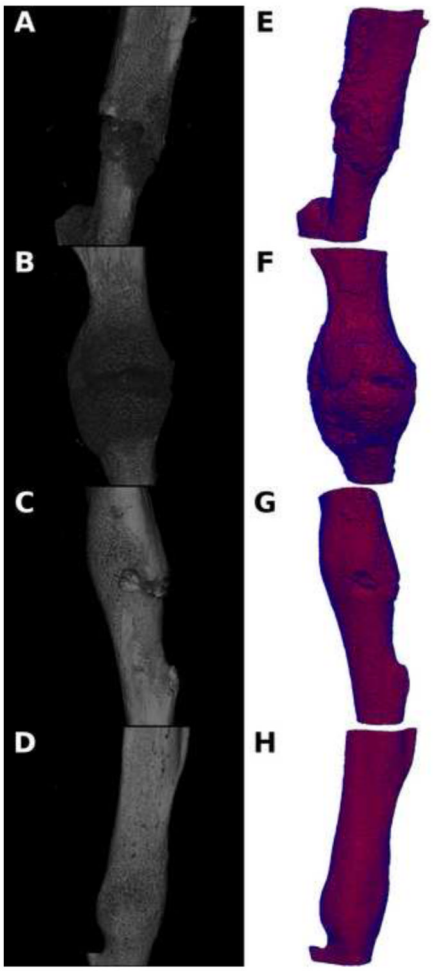

Figure 1.
Representative volumetric microCT reconstructions (A-D) and FEA meshes (E-H) of 14 days post-fracture calluses without MSC transplantation (A&E), 14 days post-fracture calluses with MSC transplantation (B&F), 21 days post-fracture calluses without MSC transplantation (C&G), and 21 days post-fracture calluses with MSC transplantation (D&H).

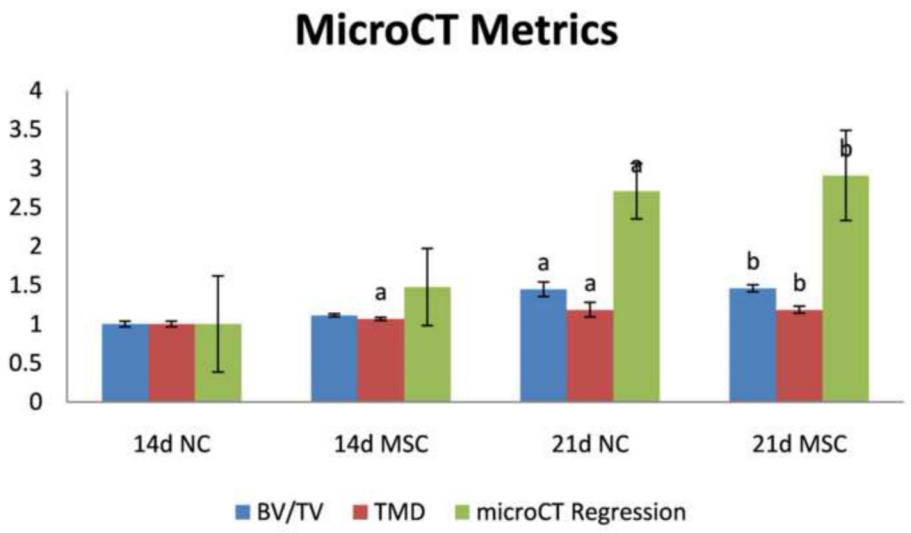

Figure 2.

MicroCT-based analysis metrics of: bone volume fraction (BV/TV), tissue mineral density (TMD), and a multi-parameter microCT-based regression that correlates microCT with biomechanical stiffness (microCT Regression) for: 14 days post-fracture calluses without MSC transplantation (14d NC), 14 days post-fracture calluses with MSC transplantation (14d MSC), 21 days post-fracture calluses without MSC transplantation (21d NC), and 21 days post-fracture calluses with MSC transplantation (21d MSC). Data are normalized with respect to data at 14d NC. Pair-wise post-test statistical comparisons are shown only for comparisons listed in bold from Table 1. [a], $p < 0.05$ vs. 14d NC. [b], $p < 0.05$ vs. 14d MSC.

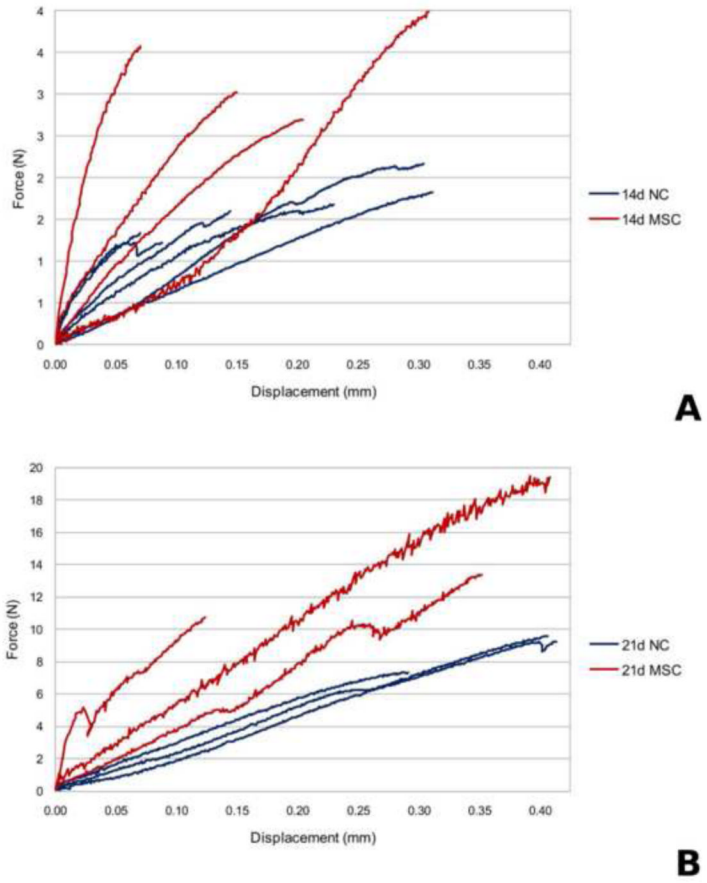

Figure 3.
Biomechanical testing force vs. displacement plot for (A) 14 days post-fracture calluses without MSC transplantation and 14 days post-fracture with MSC transplantation, (B) 21 days post-fracture calluses without MSC transplantation and 21 days post-fracture with MSC transplantation.

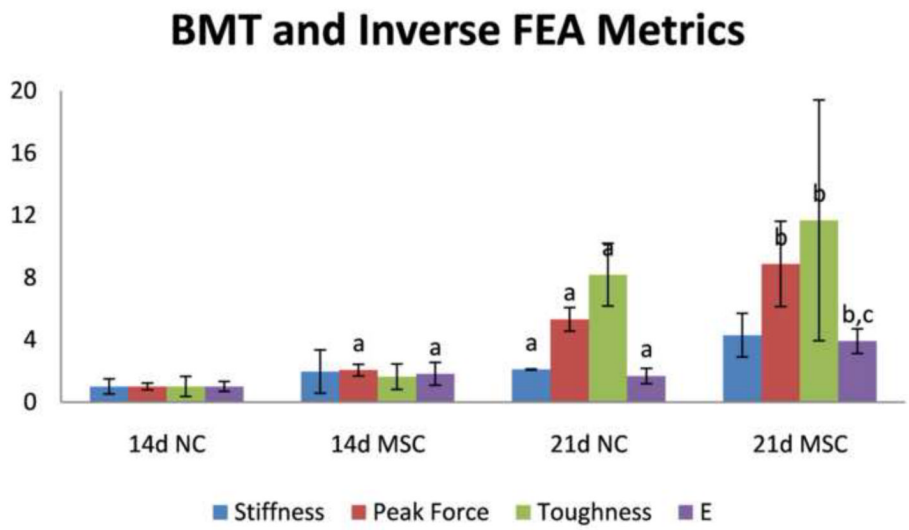

Figure 4.

Biomechanical property analysis metrics of stiffness, peak force, toughness, and inverse finite element analysis assessed elastic modulus (E) for: 14 days post-fracture calluses without MSC transplantation (14d NC), 14 days post-fracture calluses with MSC transplantation (14d MSC), 21 days post-fracture calluses without MSC transplantation (21d NC), and 21 days post-fracture calluses with MSC transplantation (21d MSC). Data are normalized with respect to data at 14d NC. Pair-wise post-test statistical comparisons are shown only for comparisons listed in bold from Table 1. [a], $p < 0.05$ vs. 14d NC. [b], $p < 0.05$ vs. 14d MSC. [c], $p < 0.05$ vs. 21d NC.

Table 1

Significance matrix comparing biomechanical testing, microCT, and inverse FEA material property reconstruction analysis metrics. The legend for each cell is shown in the upper left hand corner of the table. “E” represents the inverse FEA reconstructed modulus, “Stiffness” represents the slope of the force vs. displacement curve, “Peak Force”, represents the peak biomechanical force experienced during testing, “BV/TV” represents bone volume to total volume fraction, “μCT-Reg” represents the microCT-based stiffness multiple regression, and “TMD” represents tissue mineral density. Green denotes significant differences ($p<0.05$), while yellow represents no significant differences. P-values are reported in the matrix. Comparisons of interest are outlined in magenta, black, and red.

Cohort	**14 Day No Cells n=6**	**14 Day MSC n=4**	**21 DayNoCells n=3**	**21 Day MSC n=3**
14 Day No Cells n=6	Peak E Stiffness Force BV/TV μCT-Reg TMD			
14 Day MSC n=4	0.041 0.1526 5.00E-04 0.287 0.2336 0.012			
21 Day No Cells n=3	0.037 0.0069 2.40E-06 0.019 0.0036 0.003	6.00E- 0.8 0.8761 04 0.083 0.0161 0.052		
21 Day MSC n=3	1.00E- 04 9.00E-041.00E-04 0.003 0.003 4.00E-04	0.015 0.0794 0.004 0.005 0.0164 0.006	0.0137 0.0521 0.096 0.944 0.6317 0.924	

Table 2

Pearson product-moment correlation coefficient matrix for all metrics classified as significant by ANOVA ($p < 0.05$).

	E	Stiffness	Toughness	Peak F	BV/TV	TMD	µCT-Reg
E		0.91	0.48	0.70	0.56	0.53	0.70
Stiffness	0.91		0.48	0.69	0.62	0.57	0.75
Toughness	0.48	0.48		0.95	0.68	0.67	0.59
Peak F	0.70	0.69	0.95		0.74	0.74	0.73
BV/TV	0.56	0.62	0.68	0.74		0.86	0.83
TMD	0.53	0.57	0.67	0.74	0.86		0.76
µCT-Reg	0.70	0.75	0.59	0.73	0.83	0.76	